Journal of Molecular Liquids 356 (2022) 119040

Contents lists available at ScienceDirect

Journal of Molecular Liquids

journal homepage: www.elsevier.com/locate/molliq

Evaluation of tetracycline removal by adsorption method using magnetic iron oxide nanoparticles (Fe_3O_4) and clinoptilolite from aqueous solutions

Mehdi Rouhani [a], Seyed Davoud Ashrafi [b], Kamran Taghavi [a], Mohammad Naimi Joubani [c], Jalil Jaafari [b,*]

[a] Department of Environmental Health Engineering, School of Health, Guilan University of Medical Sciences, Rasht, Iran
[b] Department of Environmental Health Engineering, Research Center of Health and Environment, School of Health, Guilan University of Medical Sciences, Rasht, Iran
[c] School of Health, Guilan University of Medical Sciences, Rasht, Iran

ARTICLE INFO

Article history:
Received 10 October 2021
Revised 17 March 2022
Accepted 27 March 2022
Available online 1 April 2022

Keywords:
Fe_3O_4
Clinoptilolite
Tetracycline
Adsorption

ABSTRACT

In the present study, Fe_3O_4/Clinoptilolite nanocomposite was synthesized in the laboratory as a magnetic nanosorbent; mentioned nanocomposite and Clinoptilolite were employed as adsorbent for adsorption of tetracycline (TC) from aqueous solution. Structure and properties of Fe_3O_4/Clinoptilolite nanocomposite and Clinoptilolite adsorbents were detected by vibrating sample magnetometer (VSM), Fourier transform infrared spectroscopy (FTIR), energy-dispersive X-ray spectroscopy (EDAX), scanning electron microscope (SEM), X-ray diffraction (XRD) analyses. The maximum adsorption capacity (q_{max}) for Clinoptilolite adsorbent was 20.17 mg/g, while it was 180.9 mg/g for Fe_3O_4/Clinoptilolite nanocomposite. Under optimal conditions, the removal efficiency of tetracycline by Fe_3O_4/Clinoptilolite nanocomposite was 98.6%, and the highest removal efficiency was obtained at pH values of 7 and 8, which could be due to physical adsorption mechanisms such as van der Waals forces and hydrogen bonds between TC polar molecules and functional groups on Fe_3O_4/Clinoptilolite nanocomposite. The results of nanocomposite reuse study showed that Fe_3O_4/Clinoptilolite adsorbent can be reused without significant reduction in efficiency, which economically and environmentally justifies the use of Fe_3O_4/Clinoptilolite nanocomposite to remove various contaminants.

1. Introduction

Today, the indiscriminate use of antibiotics and the subsequent release of these compounds into the environment have raised concerns worldwide [1–3]. About 100,000–200,000 tons of antibiotics are consumed annually in the world [4]. Antibiotics are substances that are very useful and have many uses in medicine and veterinary medicine. However, they also have side effects. The main problem with antibiotics and drug compounds, in general, is their biological activity, which leads to adverse effects on aquatic ecosystems. The widespread presence of medicinal compounds in water, especially drinking water sources, poses a serious threat to the environment and human health [5–8]. Tetracyclines are a group of antibiotics with the general molecular formula of $C_{22}H_{24}N_2O_8$ that are widely used to treat or prevent disease and boost growth in animals and livestock, as well as to strengthen soil fertility in agriculture. If tetracycline enters the water sources, about 70–90% of it remains unchanged [9,10], so the appropriate method should be used for its treatment. Due to the high polarity and high solubility of tetracycline in water, the removal of the remaining drug is not possible by conventional methods in wastewater treatment [11].

In recent years, various methods, including biodegradation, advanced oxidation, membrane methods, electrochemical and adsorption-based methods have been used to remove tetracycline from aqueous solutions. Adsorption-based methods have many advantages over other methods, including the simplicity of design and operation, cheapness, environmental safety, and high efficiency in eliminating low concentrations of various pollutants [6,12–15].

Due to its high specific surface area and easy separation under an external magnetic field, magnetic nanoparticles have been considered as adsorbents for the separation of various pollutants from water sources [16]. Among different magnetic nanomaterials, magnetic iron oxide (Fe_3O_4) nanoparticles are widely used as adsorbents of various contaminants, especially drug residues in aqueous sources, due to their reasonable price and easy prepara-

* Corresponding author.
E-mail addresses: jalil.jaafari@yahoo.com, jalil.jaafari@gums.ac.ir (J. Jaafari).

https://doi.org/10.1016/j.molliq.2022.119040
0167-7322/

tion steps [16,17]. Magnetic iron oxide nanoparticles (Fe_3O_4) have exceptional properties and characteristics such as small particle size, high magnetic response-ability, surface performance of functional groups, biodegradability for separation and extraction of highly harmful organic substances and contaminants from water and wastewater [18]. Zeolites are among the minerals that have been widely used to remove contaminants. These materials have the three-dimensional structure of aluminosilicate. Silicon is in the form of Si (IV), and aluminum is in the form of Al (III). Negative charges are neutralized by moving cations in the network. The lattice has interconnected channels or pores that are occupied by water and cations. The cations of the lattice are mobile and this mobility provides a large adsorption property for zeolites [18]. Clintptololite zeolite with chemical formula of (Na_4K_4) (Al_8Si_4o) $O_{96}{\cdot}24H_2O$ is one of the natural adsorbents with high adsorption capacity and cheap price. They can be abundantly found in deposits of igneous, metamorphic and sedimentary and have the ability for removal of various contaminants from aqueous solutions due to its porous structure and high ion exchange [19].

Response surface methodology (RSM) is a useful model for simultaneous evaluation of combined effects of many factors influencing the responses by varying these factors simultaneously [20–24]. The Box-Behnken design (BBD) is frequently used under RSM design which consists of three interlocking 2n factorial designs having points, all lying on the surface of a sphere surrounding the center of the design. The Box-Behnken design requires a smaller number of experimental runs, maintains the good precision of the predicted response, and usually works well for process optimization.

In this study, the tetracycline (TC) removal efficiency by adsorption process using two adsorbents, i.e., Cliptitiolite and Cliptitiolite modified with magnetic iron oxide nanoparticles was evaluated and analyzed, and factors and parameters such as contaminant concentration, adsorbent, pH, etc. that may affect this process were investigated.

2. Material and methods

2.1. Chemicals

To carry out this research, chemicals including $FeCl_3{\cdot}6H_2O$, ethanol, $FeCl_2{\cdot}4H_2O$, hydrochloric acid, and sodium hydroxide used in this study were of analytical grade (98–99%) and provided by Merck Company. Tetracycline hydrochloride ($C_{22}H_{24}O_8N_2HCl$) with a purity of over 95% was purchased from Sigma-Aldrich (Germany) and was used without further purification. Cliptitiolite powder was prepared from Negin Company, Semnan, Iran.

2.2. Adsorbents preparation

In this project, the adsorbent of Cliptitiolite modified with magnetic iron oxide (Fe_3O_4) nanoparticles were prepared as follows: First step, 6 g of $FeCl_3{\cdot}6H_2O$ and 2.25 g of $FeCl_2{\cdot}4H_2O$ were added into a balloon containing 200 ml of distilled water and placed on it mixer under nitrogen gas. Next, 2 g of washed Cliptitiolite powder was added and completely stirred for one hour. After that, 20 ml of NH_4OH (25%) was added drop by drop to the solution, and the temperature of the solution was brought to 80 °C and allowed to remain at 80 °C for 2 h. The solution was then cooled to ambient temperature and the magnetized black nanoparticles were withdrawn by the magnet. These nanoparticles were washed three times with distilled water and once with ethanol. The resulting nanoparticles were withdrawn with a magnet and were placed in the oven at 80 °C for 24 h to dry. Preparation of adsorbent for magnetic iron oxide nanoparticles (Fe_3O_4) was performed by conducting all the above steps without adding Cliptitiolite powder.

2.3. Characterization of adsorbents

To determine the structure and identify organic compounds and chemical bonds and identify functional groups and molecular structure, Fourier Transform Infrared Spectroscopy (FTIR) (model: AVATAR model, made by Thermo USA) was used. To identify the crystal structure of adsorbents, X-ray diffraction (XRD) (voltage = 40kv, current = 30 mA, manufacturer: PHILIPS, made in the Netherlands) was utilized. Studying the morphology and structure of adsorbents was done by field emission scanning electron microscope (FE-SEM) made by TE-SCAN company in the Czech Republic. Identifying the composition of sample elements was performed by EDX method (device name: FESEM model MIRA III SAMX detector, made in France). Transmission electron microscope (TEM) image was recorded on a JEM-1200 EX/S, JEOL (made in Japan). In addition, VSM method was used to identify the magnetic properties of nanoparticles. Thermogravimetric analysis (TGA) was conducted using Shimadzu DTG-60 at 25 to 800 °C. The pore size distribution, specific surface area, and the pore volume of the nanocomposite were determined using the Brunauer–Emmett–Teller (BET) micrometrics (BELSORP MINI II, Japan).

2.4. Experimental design and optimization

To design the structure of contaminant adsorption tests (tetracycline) by Fe_3O_4/Clinoptilolite nanosorbents, BBD and RSM design expert statistical software were used.

The variables used in this study were given in Table 1. Data analysis was performed with a significance level of 95% for the desired response of ‘‘removal of TC contaminant”. The level of each variable was previously determined by testing. Adsorption experiments were performed as follows: initially, 200 mg of tetracycline powder was prepared by adding 200 mg/L stock solution to one liter of distilled water and completely dissolved. Adsorption experiments were performed using batch system and inside 250 ml Erlenmeyer flask containing 200 ml of certain concentrations of TC at different pH, temperature, and contact times. The samples were then placed in a shaker at 240 rpm for proper mixing of the adsorbent and adsorbate. At the end, the adsorbent was separated from the solution by centrifugation, and the residual antibiotic concentrations were measured using the UV–Visible spectrophotometer (CE CECIL) at the maximum wavelength of the TC absorption wave (362 nm). The pH of the solutions was also adjusted using 0.1 M hydrochloric acid (HCL) and 0.1 M sodium hydroxide (NaOH). Each test step was repeated twice, and their average was presented as the final results. The amount of tetracycline adsorbed on the adsorbent and the removal efficiency were calculated through Eqs. (1) and (2). In mentioned relations qe (mg/g) is the amount of tetracycline adsorbed on the adsorbent at equilibrium time; C_0 (mg/L) and C_e (mg/L) are the concentration of the contaminant (tetracycline) at the initial time and equilibrium time; m (g) is the adsorbent mass; (L) V is the volume of the solution, and (%) R is the amount of contaminant removal efficiency (tetracycline) by the adsorbent.

$$qe = \frac{(C_{0-}C_e)}{m}V \tag{1}$$

$$R = \left(\frac{C_0 - C_e}{C_0}\right) \tag{2}$$

Table 1
Experimental independent variables.

Variables	Factor	Range and level		
		−1	0	+1
pH	*A*	5	7	9
Adsorbent dosage (g/L)	*B*	0.3	1.00	1.7
Tetracycline concentration (mg/L)	*C*	10	55	100

2.5. Adsorption isotherms

Adsorption isotherms of equilibrium data are used to describe how the adsorbent reacts with the adsorbate (tetracycline). Isotherms actually express the adsorption capacity of an adsorbent. In this study, Langmuir, Freundlich, Temkin, Sips, and Redlich-Peterson isotherms were used to investigate and analyze the experimental data and characterize the equilibrium state in the adsorption process between solid and liquid phases. The Langmuir isotherm indicates the adsorption of a uniform layer of adsorbent with equal energy on all adsorbent surfaces and states that all adsorption sites have the same coherence with the adsorbent molecules and the transfer process does not occur from the adsorbate surface to the adsorbent surface. The Freundlich isotherm is based on the multilayer, non-uniform and heterogeneous adsorption of adsorbates on the adsorbent. The nonlinear equation of these two equilibrium isotherms is expressed as follows [25]:

Langmuir isotherm

$$q_e = \frac{q_m C_e k_L}{1 + C_e k_L} \tag{3}$$

Freundlich isotherm

$$q_e = k_f {c_e}^{1/n} \tag{4}$$

In these equations, C_e (mg/L) is the equilibrium concentration of tetracycline; q_e (mg/g) is the amount of TC adsorbed on the adsorbent at equilibrium; q_m (mg/g) is maximum adsorption capacity; k_L (mg/L) is constant Langmuir; the k_f is Freundlich constant, and the n is Freundlich isotherm constant depends on the adsorption intensity.

In the Temkin isotherm model, the adsorption energy, as well as the interaction between the adsorbate and the adsorbent, are indirectly expressed, and it is assumed that the heat of adsorption of all molecules in a layer decreases linearly with the coating of molecules due to repulsion between similar adsorbate ion and the adsorption process on the adsorbent is uniform:

Temkin isotherm

$$q_e = B_l \ln k_T C_e \tag{5}$$

In this equation, $B_l = Rt/b$, R and T are the temperature (k°) and the global constant of gases, respectively; b (KJ⁄mol) is constant of Temkin; B_l (L⁄mol) is energy constant of isotherm isotherm and K_T $(1/min)$ is constant of Temkin isotherms [25].

The Sips isotherm model at low adsorbent concentrations can be used for heterogeneous adsorbent surfaces and confirms the Freundlich isotherm at low adsorbent concentrations, while at high adsorbent concentrations, it describes the monolayer adsorption and the Langmuir isotherm and its equilibrium equation is as follows.

$$q_e = \frac{k_L c_e^{n_L}}{1 + (a_L c_e)^{n_L}} \tag{6}$$

In this equation, $k_l(L/GR)$ is the constant of the Sips isotherm, nL is the representative of the Cips isotherm, and a_L (L/GR) is the constant of the Cips isotherm.

The Redlich-Peterson isotherm is a hybrid three-variable isotherm, which combines both the properties of the Freundlich and Langmuir isotherms. Its equilibrium equation is given in Eq. (7).

$$q_e = \frac{k_R c_e}{1 + (a_R C_e^g)} \tag{7}$$

In the above equation, $k_R(L/GR)$ is constant of Redlich - Peterson isotherm,a_R is a constant value and g ($0 < g < 1$) is the power and indicates the degree of heterogeneity of the adsorbent.

2.6. Adsorption kinetic

The adsorption kinetic is used to describe the transfer behavior of adsorbate molecules on the adsorbent per unit time and to investigate the variables affecting the reaction rate of adsorption kinetics relationships. In most cases, pseudo-first-order and pseudo-second-order kinetic models are used to express the kinetic behavior of pollutant adsorption on various nanosorbents. The nonlinear state of these relations is expressed in Eqs. (8) and (9):

$$\text{Pseudo} - \text{first} - \text{order} \quad q_{t=} q_e\left(1 - exp^{-k_1 t}\right) \tag{8}$$

$$\text{Pseudo} - \text{second} - \text{order} \quad q_t = \frac{q_e^2 k_2 t}{1 + q_e k_2 t} \tag{9}$$

In these equations, q_e (mg/g) is the adsorption capacity at equilibrium, qt (mg/g) is the absorption capacity at time t, and k1 and k_2 are the rate coefficient (1/min). Elovich equation is also widely used to study the kinetics of different reactions, which describes the chemical adsorption reaction in nature; the nonlinear equation is expressed in Eq. (10) [26].

$$Q_t = \frac{1}{\beta} \ln(\alpha\beta) + \frac{1}{\beta} \ln t \tag{10}$$

In the above equation, Q_t is the amount of contaminant adsorption at time t, α (g/μg.H) is initial adsorption rate, and β (g/μg.H) is desorption constant during the test time.

2.7. Effect of temperature

To determine the thermodynamic parameters of the adsorption of pollutants (tetracycline) by the nanosorbents used, thermodynamic studies are performed. Determining thermodynamic parameters is important to determine whether the design is endothermic or exothermic. The effective factors that should be quantified in thermodynamic studies are standard free energy (ΔG°), standard enthalpy (ΔH°), and standard entropy (ΔS°), which are calculated using the following equations:

$$\frac{\Delta H^{\circ}}{RT} - \frac{\Delta S^{\circ}}{R} = \ln k_d \tag{11}$$

$$k_d = \frac{q_e}{c_e} \tag{12}$$

$$\Delta G0 = -RT\ln KL \tag{13}$$

In these equations, R (8.314 J/mol.°K) is universal constant of gases; T is (solution temperature, °K); Kd (L/g) is ratio of the amount of TC adsorbed on the adsorbent to the amount remaining in the solution. ΔH° and ΔS° are obtained by slope and intercept the line obtained from drawing $\ln k_d$ versus 1/T. Experiments to determine the isotherms, kinetics, and thermodynamic parameters and to investigate the effect of interfering ions and reusability of adsorbent were done as three replication.

3. Results and discussion

3.1. Characterization of adsorbents

3.1.1. XRD analysis

X-ray diffraction (XRD) diagrams of Clinoptilolite and Fe_3O_4, Fe_3O_4/Clinoptilolite adsorbents in Cu-Kα radiation at 25 °C were compared in Fig. 1. The pattern in Fig. 1 (a) is for Clinoptilolite adsorbent; it shows that it has several peaks at 2θ = 32.00, 30.02, 28.1, 26.15, 22.40, 17.38, 11.22, and 9.89, which is corresponded to the XRD pattern of the reference sample (JCPDS: 00-025-1349) [19,27]. Also, in Fig. 1 (b), the XRD pattern of the Fe_3O_4 adsorbent shows that it has several peaks at 2θ = 71.1, 62.39, 58.00 44.4, 43.34, 36.2, 34.32, 30.5, and 29.5. By matching the XRD pattern of the Fe3O4 adsorbent with the XRD pattern of the reference sample (adsorbent synthesized by Yan Wei et al.), the crystal and cubic structure of this adsorbent was confirmed (JCPDS: 19-0629) [28]. In the study of the structure of Fe_3O_4/Clinoptilolite nanocomposite represented in Fig. 1 (c), the presence of seven peaks at 2θ = 22.5, 30.5, 32, 34, 43, 58.5, and 62° was detected. Using XRD analysis, the complete formation of Fe_3O_4/Clinoptilolite was conformed due to the absence of hematite peaks and the absence of metal hydroxides and other impurities as well as the presence of long and sharp peaks [29]. Moreover, through Eq. (14) which is called Scherrer, the diameter size of the nanoparticles was calculated [29]:

$$D = \frac{k\lambda}{\beta \mathrm{Cos}\theta} \tag{14}$$

In this equation, D is the diameter of the nanoparticles, k is a constant coefficient equal to 0.89, θ is the diffraction angle at the main peak, λ is the radiation wavelength at Cu-Kα, and β is the width of the main peak at half its height.

3.1.2. Fourier transform infrared spectroscopy

Fig. 2 shows the FTIR spectrum of Fe_3O_4/Clinoptilolite, Fe_3O_4 and Clinoptilolite adsorbents in the range of 4000–1400 cm. In FTIR of Clinoptilolite adsorbent (Fig. 2a), peak at 1069.61 cm^{-1} is related to asymmetric stretching vibrations of Si-O-Si and Al-O-Al bonds. Also, the peaks of 796.07 and 468.75 cm-1 are due to the symmetrical stretching vibrations of the Si-O and Al-O bonds in the Si-O-Si and Al-O-Al joints, and the peaks at 1635 and 3434 bonds are due to the O-H bonds related to the water molecule [6]. In the FTIR spectrum of Fe_3O_4 adsorbent (Fig. 2a), the specified peak in the range of 480–580 cm^{-1} is related to the Fe-O bond [30]. The FTIR spectrum of Fe_3O_4/Clinoptilolite nanocomposite (Fig. 2c) shows that most peaks in the FTIR spectrum of the clinoptilolite nanocomposite are also observed in the Fe_3O_4/Clinoptilolite nanocomposite spectrum. Also, in comparison with the FTIR spectrum of Fe_3O_4 adsorbent (Fig. 2a), the presence of a peak in the range of 480–580 cm^{-1} related to Fe-O bonding was detected in the FTIR spectrum of Fe_3O_4/Clinoptilolite nanocomposite. The adsorbent structure of Fe_3O_4 remains unchanged in the composition of Fe_3O_4/Clinoptilolite nanocomposite, which is consistent with the results of the study of Mollahosseini et al. [30].

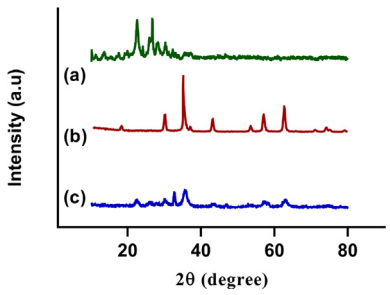

Fig 1. XRD diagram of adsorbents of Clinoptilolite (a), Fe_3O_4 (b) and Fe_3O_4/Clinoptilolite nanocomposite (c).

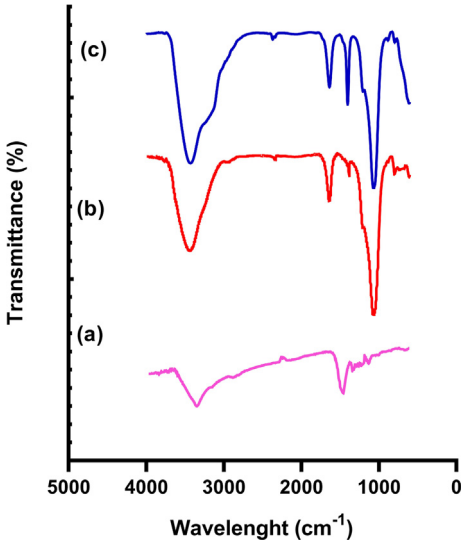

Fig 2. FTIR diagram of adsorbents of, Fe_3O_4 (a), Clinoptilolite (b) and Fe_3O_4/Clinoptilolite nanocomposite (c).

3.1.3. Vibrating-sample magnetometer (VSM) analysis

To measure the magnetic properties of the synthesized adsorbents, the Vibrating Sample Magnetometer (VSM) test was performed at 25 °C, and the corresponding hysteresis curve was prepared by changing the magnetic field (H) in the range of 15000+ and −15000 (Oe) (Fig. 3). The saturation magnetization (Ms) of the magnetite sample (Fe_3O_4) at room temperature was estimated to be 49.5 $emu.g^{-1}$, which was significantly reduced to 30.00 $emu.g^{-1}$ for the Fe_3O_4/Clinoptilolite sample. The decrease in saturation magnetization in the zeolite-coated magnetite sample is due to the placement of the Clinoptilolite coating on the magnetite. Residual magnetization and negligible magnetic induction in the results also indicate that the magnetic nanoparticles are super paramagnetic in both samples, which is achieved by converting the hysteresis ring to an S-shaped curve [31]. Also, both adsorbents were separated from the prepared liquid solutions by the external magnet in less than 20 s.

The Fe_3O_4/Clinoptilolite magnetic nanoparticles were determined by BET analysis using N_2adsorption method, which is reported in Table S1 and Fig. 3c. The textural properties, i.e the average pore diameter, special surface area, and the total volume pores of the synthesized composite were 5.43 nm, 165.71 m^2/g, and 74.56 and 0.387 cm^3/g, respectively. The average pore size of adsorbent was found to be in range of 1–7.43 nm. Based on the IUPAC category, the shape of this isotherm is type II, which the adsorption increases sharply at relatively low pressures.

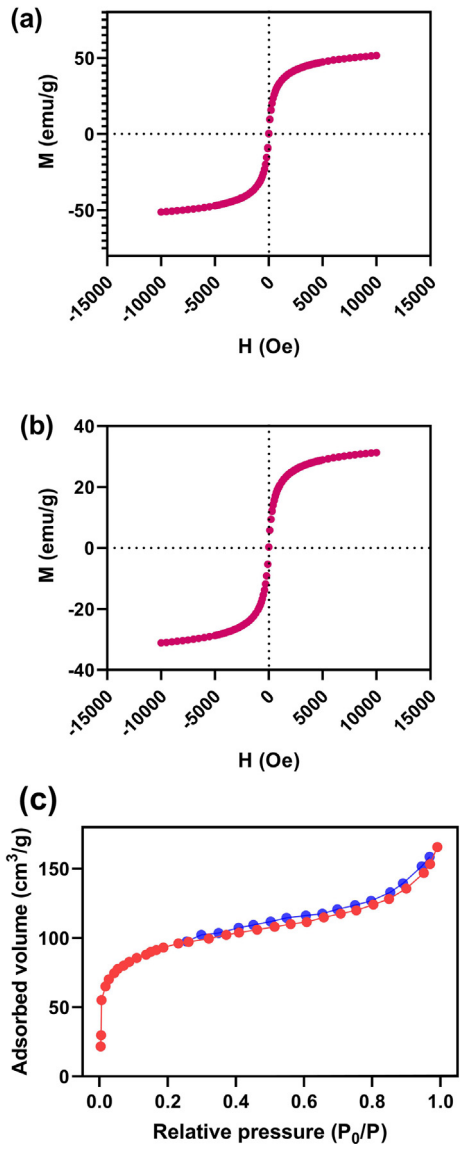

Fig. 3. The diagram of the magnetic value of Fe_3O_4 (a), Fe_3O_4/Clinoptilolite nanocomposite (b) and BET of Fe_3O_4/Clinoptilolite nanocomposite (c).

3.1.4. SEM and TEM analysis

Fig. 4a shows SEM images of Clinoptilolite adsorbent, and Fig. 4b shows images of Fe_3O_4/Clinoptilolite magnetic nanoparticles adsorbent. By matching the size of the nanoparticles mentioned with the scale below these images, the particle size of these adsorbents can be measured. As can be seen in Fig. 4a, Clintptololite zeolite powders with an average size of less than 50 nm can be detected as separate particles or as larger masses. However, in Fig. 4b, the scanning electron microscope (SEM) presents the image of Fe_3O_4/Clinoptilolite magnetic nanosorbent as a uniform spherical particle with an average size of less than 60–80 nm due to the presence of clinoptilolite in the composition of Fe_3O_4/Clinoptilolite nanocomposite. The porosity created on the nanocomposite has been able to create many sites for the adsorption and removal of various contaminants [32]. Fig. 4c shows the TEM image of Fe_3O_4/Clinoptilolite nanocomposite; as shown, sample is visible in the TEM image of magnetic Fe_3O_4/Clinoptilolite nanocomposite nanoparticles coated on the iron oxide nanoparticles, which is in a darker color base on the 50 nm scale of the image.

3.1.5. EDX analysis

The EDAX spectra of Fe_3O_4/Clinoptilolite, Fe_3O_4, and Clinoptilolite adsorbents were presented in Fig. 5. The weight percentages of O, Na, Mg, Al, Si, K, Fe, Sr, and Ba were 48.79, 1.48, 0.53, 6.36, 27.31, 0.96, 0.77, 26.58, and 1.12%, respectively. In Fe3O4 adsorbent, the weight percentages of Cl, O, Al and Fe elements in EDAX analysis were 4.61, 46.7, 0.59, and 48.23%, respectively. In Fe_3O_4/Clinoptilolit adsorbent, the weight percentages of the constituents of this nanosorbent were reported as follows: O = 34.93, Fe = 44.58, Na = 0.41, Al = 3.17, Si = 11.29, Sr = 1.07, and Ba = 1.61%; this indicates the synthesized adsorbent of the above elements. Table 2 compares the weight percentage of adsorbent elements used in this study with chitosan/clinoptilolite/magnetite nanocomposite [33] and generally corresponds to the weight percentage of Fe_3O_4/Clinoptilolit nanocomposite elements.

3.1.6. Thermogravimetric analysis (TGA)

Thermal strength and stability of synthesized materials were analyzed by thermogravimetric analysis (TGA) (from 25 °C to 800 °C by the heating rate of 10 °C/min). As shown in Fig. 6 a, for pure Fe_3O_4, total weight loss of 4.3% may be attributed to the loss of water when the temperature increase from 40 °C to 800 °C. In addition, a small exothermic peak appears in the range from 550 °C to 600 °C, which corresponds to the phase transition from Fe_3O_4 to α-Fe_2O_3 [34,35]. As shown in Fig. 6 b and c, at 40 to 150 °C, there was a small loss of weight due to the loss of physically adsorbed water in the material of Clinoptilolite and Fe_3O_4/Clinoptilolite. The two latter weight losses (150–300 °C and 300–800 °C) were attributed to crystal structure changes during the thermal treatment process.

3.2. Modeling and optimization of the adsorption process by statistical methods

Table S2 represents the actual values of the removal efficiency of tetracycline contaminant by Fe_3O_4/Clinoptilolite nanosorbent

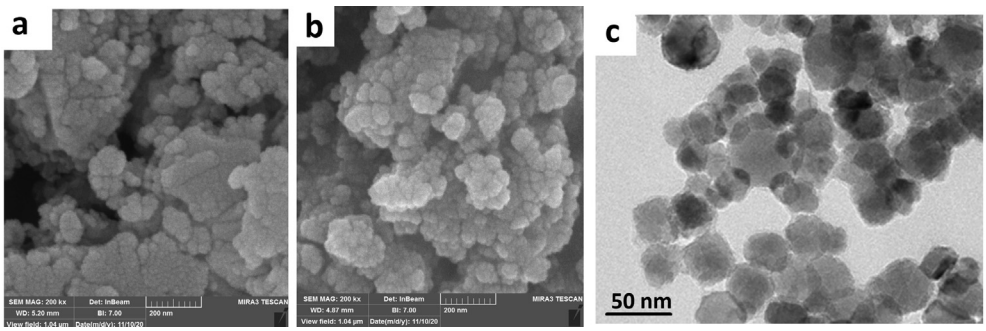

Fig. 4. SEM image of adsorbent Clinoptilolite (a) and SEM (b) and TEM (c) of Fe_3O_4/Clinoptilolit nanocomposite.

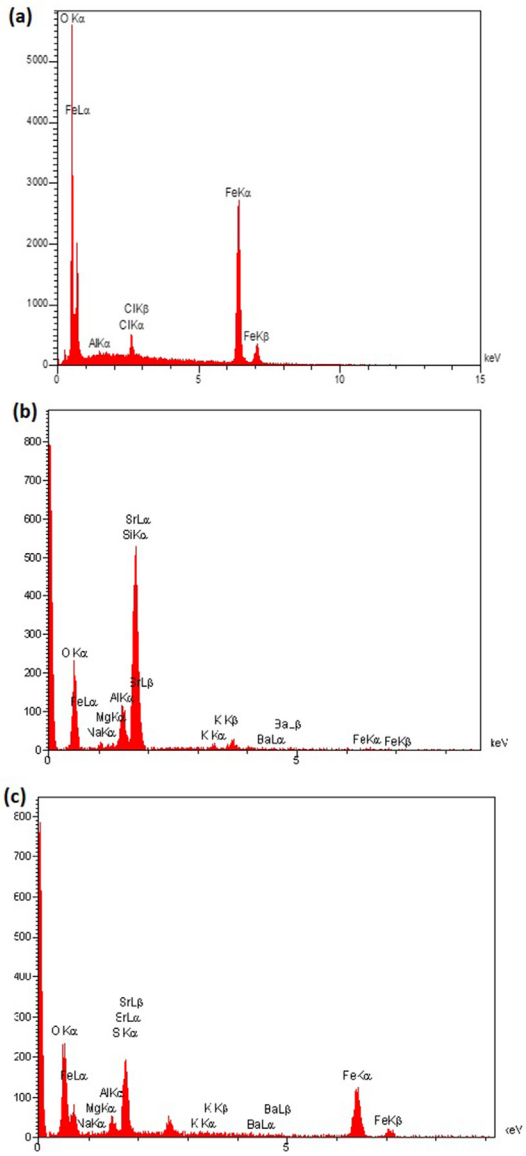

Fig. 5. EDX spectrum of Fe_3O_4 (a), Clinoptilolit (b) and Fe_3O_4/Clinoptilolit nanocomposite (c).

as well as the removal efficiency predicted by the model, which shows that the proposed model data are quite close to the actual values, and there is a good correlation between actual results and predicted values (R^2 = 0.995).

Using the response surface methodology, the quadratic model, Eq. (15), was obtained to predict the removal efficiency, and this equation (Eq. (15)) shows the experimental relationship between the tested variables and the removal efficiency.

$$R(\% (= -232.573 + 84.10801A + 35.04189B0.06096C + 1.42857AB + 0.066667AC + 0.105556BC - 6.21987A^2 - 12.2541B^2 - 0.00593C^2 \quad (15)$$

In this equation A, B, C are pH, adsorbent dose and initial concentration of TC, respectively.

The results obtained from the design of the experiments were analyzed using the statistical test of analysis of variance (ANOVA) at the confidence level of 95%, the results of which were shown in Table S3 and Fig. 6d. The importance of each variable or its interaction with other variables is determined by *p-value* and *F-value*, so that if the *p-value* is less than 0.05 or F-value is more than 4–5, that variable or model is effective and significant, and if the *p-value* is more than 0.1 or *F-value* is less than one, the variable is practically ineffective and is excluded. According to the information in the table, the *F-value* of the model is 160.4 and the *p-value* of the model is 0.0001, which indicates that the model is acceptable. Among the different models proposed, quadratic equation model experimental design software due to greater compatibility with the data.

In this model, in addition to the individual effect of each of the variables, the interaction between different variables was also investigated. According to the *p-value* values listed in Table 4, the expressions including A (pH), B (adsorbent dose), C (TC Concentrate), AC, BC, A^2, B^2, and C^2 are meaningful. Finally, Eq. (15) was expressed as a coded quadratic equation. Also, in the Lack of fit test, the value of *P-value* = 0.1238 and *F-value* = 3.6 means that the model fits the experimental data well and there is no outdated data in the model. Examining the ANOVA table, the proposed equation, and Pareto chart in Fig. 6d, it can be seen that the order of effectiveness of the parameters is the absorbent dose > contaminant concentration > pH. Also, the order of effectiveness of the interactions is in the form of contaminant concentration-pH < Contaminant concentration-adsorbent dose < pH-adsorbent dose. In addition to the information in the analysis of the variance table, the values for the R^2, Adj R^2, and Adeq R^2 also help to verify the validity of the proposed model. The value for R^2 of the model is 0.9952, which indicates that 99.52% of the data changes are expressed by the model. Also, the value of 0.989 for Adj R^2 indicates a high degree of correlation and consistency between the actual and predicted response values. In addition, the value of Adeq precision = 33.6523 indicates that the model is satisfactory.

3.3. Investigation of the effect of variables on the removal of tetracycline by Fe_3O_4/Clinoptilolite adsorbent

3.3.1. Effect of pH

TC is an amphoteric organic substance that according to the pH of the solution, is observed in the forms of (a) TCH_3^+ at pH < 3.3 and (b) TCH_2° at 3.3 < pH < 7.7 and (c) TCH^- at 7.7 < pH < 9.7 and TC^{2-} (d) at pH > 9.7 in aqueous solutions. The pH of the zero charge (pHzpc) of Fe_3O_4/Clinoptilolite adsorbent is in the range of pH of 5.5 to 6.5 [36,37], which indicates that the charge of the nanocomposite surface is positive in the range of less than this pH and protonated and is negative in the pH values higher than this pH. In this

Table 2
Optimum conditions predicted by software (results from three replicate values).

Variables	Lower limit	Upper limit	Optimum value	Response (%)	
				Actual	Predicted
A: pH	3	10	7.5	98.8	100.00
B: TC concentration (mg/L)	10	100	50.00		
C: Adsorbent dose (g/L)	0.3	1.7	1.5		

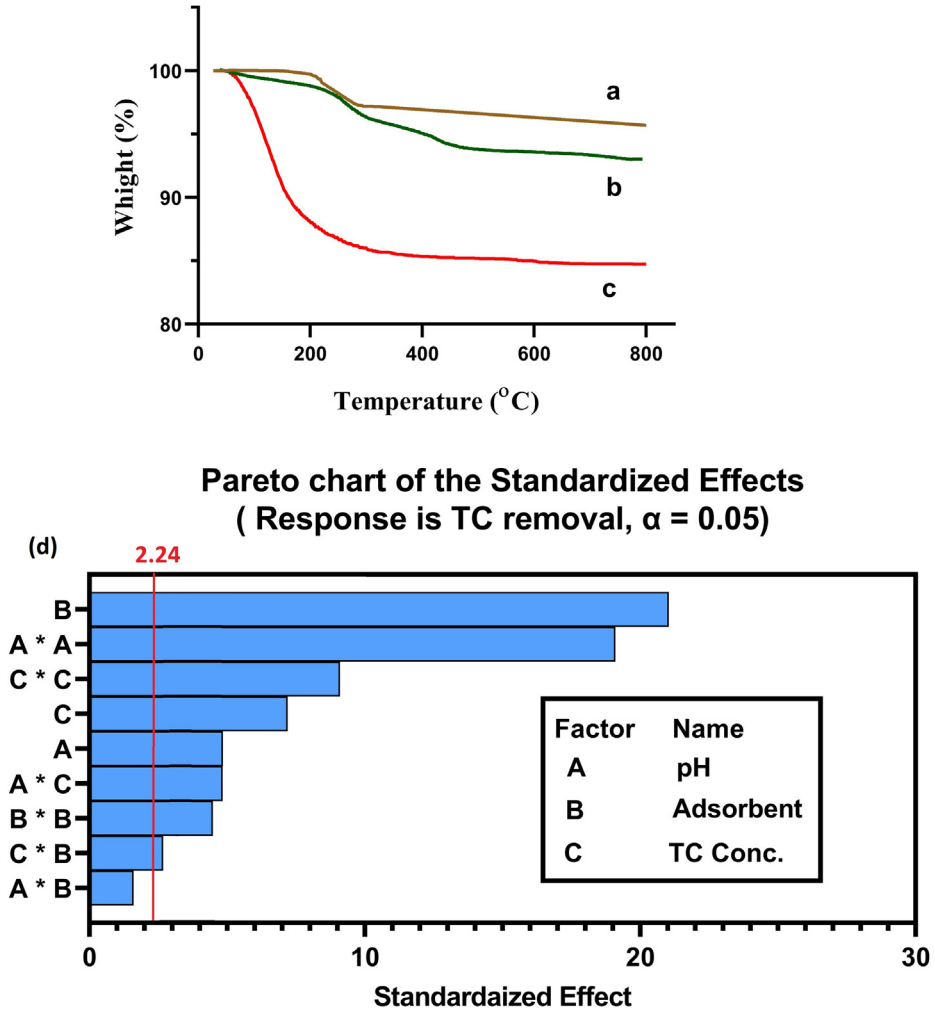

Fig. 6. TGA thermograms of Fe_3O_4 (a), Fe_3O_4/Clinoptilolit nanocomposite (b) and Clinoptilolit (c) Pareto chart of the standardized effects (d).

study, the removal of TC by Fe_3O_4/Clinoptilolite adsorbent was investigated at pH values between 3 and 10 (Fig. 7 a and b) and the highest removal efficiency was obtained at pH values of 7 and 8. At pH of 3, the percentage of contaminant removal was low and zero due to the repulsive force between the positive electric charges of the pollutant and the adsorbent surface. With increasing the pH from 5 to 7, the removal efficiency increased, so that 74% of the contaminant was removed in the conditions including adsorbent dose of 1.7 g/L and contaminant concentration of 55 mg/L. Furthermore, 97.1% of the contaminant was removed by Fe_3O_4/Clinoptilolite nanocomposite at pH of 7, adsorbent dose of 1.7 g/L, and contaminant concentration of 10 mg/L. As can be seen in the Fig. 7 a and b, it was the highest TC removal efficiency observed. Given that the TC molecule is electrically neutral in the range of 3.3 < pH < 7.7, and the electrostatic gravitational forces alone can not justify the high removal efficiency in this range, physical adsorption mechanisms such as van der Waals forces and hydrogen bonds between TC polar molecules and functional groups on the surface of Fe_3O_4/Clinoptilolite nanocomposite can indicate high adsorption efficiencies at pH of 7 and 8 [6]. With increasing pH, the amount of negative ions from TC (anions) prevails in solution at pH of 9; this leads to an electrostatic repulsion force between the same charges (negative-negative) and further decrease in the removal efficiency due to presence of the negative charges on the nanocomposite surface. In the study conducted by Babaei, the highest removal efficiency of TC by Magnetic Hydroxyapatite was obtained at pH values of 7 and 8, which is consistent with the results of this study [38].

3.3.2. Effect of initial tetracycline concentration

The effect of initial concentration of TC on the removal of contaminants by Fe_3O_4/Clinoptilolite nanocomposite was investigated using three concentrations of contaminants in the range of 10–100 mg/L at pH of 5–9 and adsorbent dose of 0.3–1.7gr/L, and the results were reported in Fig. 7a and c. At a concentration of 10 mg/L and a pH of 7, 97.1% of the contaminant was removed. With increasing the initial concentration of the contaminant at an initial concentration of 100 mg/L, the removal efficiency reached 93.4%; these results show that with increasing the initial concentration of contaminants, the adsorption efficiency decreases due to the saturation of the adsorbent surface and the occupation of nanocomposite adsorption sites at high concentrations of TC and the increase in contaminant residues after adsorption [39]. These results are consistent with the study of A, Dehghan et al. for the removal of TC by the zeolitic adsorbent imidazolate [6]. The adsorption capacity of Fe_3O_4/Clinoptilolite nanocomposite for the initial concentration of 10 mg/L was obtained to be 9.7 mg/L, however, it was found to be 93.4 mg/L at the initial concentration of 100 mg/L. This increase in pollutant adsorption capacity is achieved by increasing the initial concentration of TC due to the increase in repulsive force due to the increase in the number of pollutant molecules and the pollutant concentration gradient [6].

Table 3
Isotherm parameters for tetracycline adsorption by Clinoptilolite and Fe_3O_4/Clinoptilolite nanocomposite.

Isotherm model	Parameter	Clinoptylolite	Fe_3O_4/Clinoptilolite nanocomposite
Experiment	q_{max} (mg/g)	20.17	180.9
Langmuir	q_{max} (mg/g)	20.17	178.7
	K_L (L mg^{-1})	0.0012	0.065
	R^2	0.971	0.988
	RMSE	1.72	10.33
Freundlich	q_{max} (mg/g)	18.65	180.9
	N	2.67	1.73
	K_F (L mg^{-1})	29.59	31.94
	R^2	0.958	0.997
	RMSE	2.09	4.01
Temkin	q_{max} (mg/g)	17.24	155.8
	B_1	476	72.8
	K_T (L mg^{-1})	0.152	4.89
	R^2	0.969	0.942
	RMSE	1.78	20.29
Sips	q_{max} (mg/g)	18.79	181.2
	k_L	0.468	31.98
	n_L	0.772	0.566
	a_L	0.007	0.007
	R^2	0.999	0.997
	RMSE	0.13	3.99
Redlich-peterson	q_{max} (mg/g)	19.09	180.9
	K_R/(L g^{-1})	2891	3035
	a_R/(L $mmol^{-1}$)	4324	94.1
	g	0.355	0.424
	R^2	0.999	0.997
	RMSE	0.4	4.63

Table 4
Comparison of the adsorption of tetracycline by Clinoptilolite and Fe_3O_4/Clinoptilolite nanocomposite and other reported adsorbents.

Adsorbent	q_{max} (mg/g)	Reference
Fe_3O_4/Clinoptilolite	180.9	This study
Clinoptilolite	20.17	This study
Magnetic Hydroxyapatite	64.4	[38]
Magnetic polyurethane polymer nanocomposite	13.17	[53]
Chitosan	41.67	[54]
Cu-immobilized alginate	53.29	[51]
pistachio shell powder coated with zinc oxide nanoparticles	98.717	[55]
magnetic rice straw derived biochar	98.314	[56]

The results of this part of the study are consistent with the results of Mirsoleimani-azizi et al. for the removal of tetracycline by MOF-5 adsorbent [40].

3.3.3. *Effect of adsorbent amount (dose) on the adsorption process of tetracycline by Fe_3O_4/Clinoptilolite nanocomposite nanosorbent*

In order to investigate the effect of the amount (dose) of adsorbent on the TC adsorption process by Fe_3O_4/Clinoptilolite nanocomposite, experiments were designed and performed with TC values of 50 mg/L and pH of 5–9 and adsorbent values of 0.3–1.7 g/L, and its results were represented in Fig. 7b and c. Removal of TC using the adsorbent amount of 0.3 g/L was in range of 42–66% for different concentrations of contaminants. With increasing the adsorbent dose to 1.7 g/L, the removal efficiency of the contaminant increased from 74 to 97.1% for different concentrations of contaminants; this increase in efficiency is described by the increase in the number of adsorption sites on the adsorbent surface due to the increase in the amount of adsorbent and more access of contaminant molecules to the adsorbent pores. With increasing the adsorbent dose, in high adsorbent amounts, the contaminant

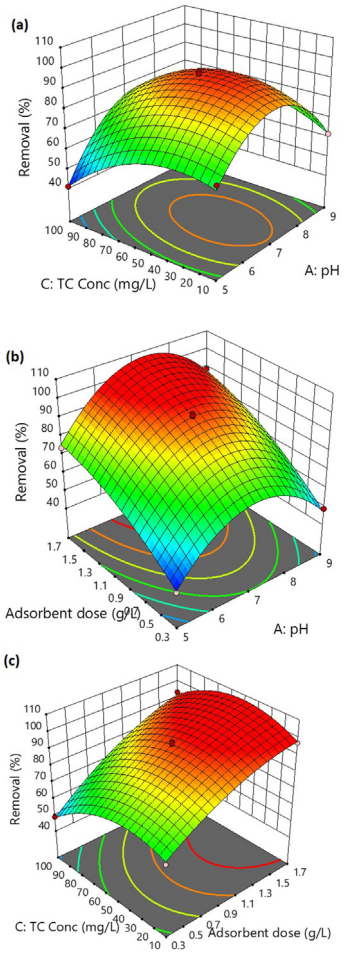

Fig. 7. Effect of pH, adsorbent dose and tetracycline concentration on tetracycline removal by Fe_3O_4/Clinoptilolit nanocomposite.

removal efficiency remains almost constant due to the reduction in the number of contaminant molecules in high adsorbent doses and the limitation of the number of contaminant molecules, which should be adsorbed and removed [35]. In the study of Mirsoleimani-azizi et al., the removal efficiency of TC by MOF-5 was increased by increasing adsorbent dose [40].

3.4. *Optimization studies of operational variables*

In the optimization process, the main goal is to find a combination of the levels of variables used in which the maximum adsorption efficiency of TC by Fe_3O_4/Clinoptilolite nanocomposite is achieved. To determine the optimal adsorption conditions in the desired range for each factor, numerical optimization of DISGN Expert software was used. Optimal conditions obtained by the software to achieve the maximum removal rate consisted of three variables, the best of which (based on usefulness) are presented in Table 2. The removal rate achievable in the desired conditions is predicted by the software.

Experiments were performed under optimal conditions with two repetitions and the average value of the results of these experiments is reported in Table 5, which obtained results for pollutant removal efficiency by Fe_3O_4/Clinoptilolite nanocomposite were very close to predicted values that confirms the validity and adequacy of the model. The amount of error obtained also indicates the high accuracy and precision of the predicted model.

Table 5
Results of thermodynamic studies under conditions including pH: 8, adsorbent dose of 1 g/L and tetracycline concentration of 50 mg/L.

Concentration (mg/L)	Temperature (K) ΔG (kJ/mol)					ΔH (kJ/mol)	ΔS (kJ/mol)
	298	303	308	313	323		
50	−7.34	−7.35	−6.14	−5.14	−3.68	−54.91	−0.15

3.5. Adsorption isotherms

The results of Langmuir, Freundlich, Temkin, Sips and Redlich-Peterson adsorption isotherms for adsorption of TC by Fe_3O_4/Clinoptilolit and Clinoptilolite adsorbents are given in Table 3 and Fig. 8, respectively. The results from removal of the TC by Clinoptilolite adsorbent show that considering the higher correlation coefficient (R^2) and less RMSE (root-mean-square error) is good consistent with the Sips isotherm and this process is homogeneous. Moreover, the removal process by Fe_3O_4/Clinoptilolite nanocomposite, considering correlation values of R^2 and RMSE, is correlated with Freundlich, with a coefficient of determination of R^2 = 0.997. Because the R^2 of Freundlich isotherm is higher and has less RMSE error than other isotherms; this indicates that the adsorption sites of this nanocomposite are not homogeneous and are different from each other and the structure of this nanocomposite is heterogeneous and absorbent.The maximum adsorption capacity (q_{max}) for Clinoptilolite adsorbent in the adsorption of the adsorbate according to the Langmuir isotherm is 20.17 mg/g.

The adsorption of TC on Clinoptilolite is a complex process consisting mainly of ion exchange and adsorption, and according to similar studies on Clinoptilolite, it could be accompanied by precipitation, particularly at higher initial concentrations [39,41]. The complexes of functional groups formed on the surface and TC can be sorbed on particle surface sites of different sorption affinity. The surface charge remaining after detachment of surface framework bonds is non-homogeneously distributed over the particle and represents a newly formed active site suitable for the adsorption of pollutants [42]. Results obtained from the present study had a trend similar to the study conducted for the adsorption of Congo red dye from aqueous solution by calcium-rich volatile ash [43], the study of Fil et al. (2014) for adsorption of Violet 16 dye adsorption using Monte Morillont [44], and study performed for adsorption of Arsenic and dexamethasone using Clinoptilolite [45,46].

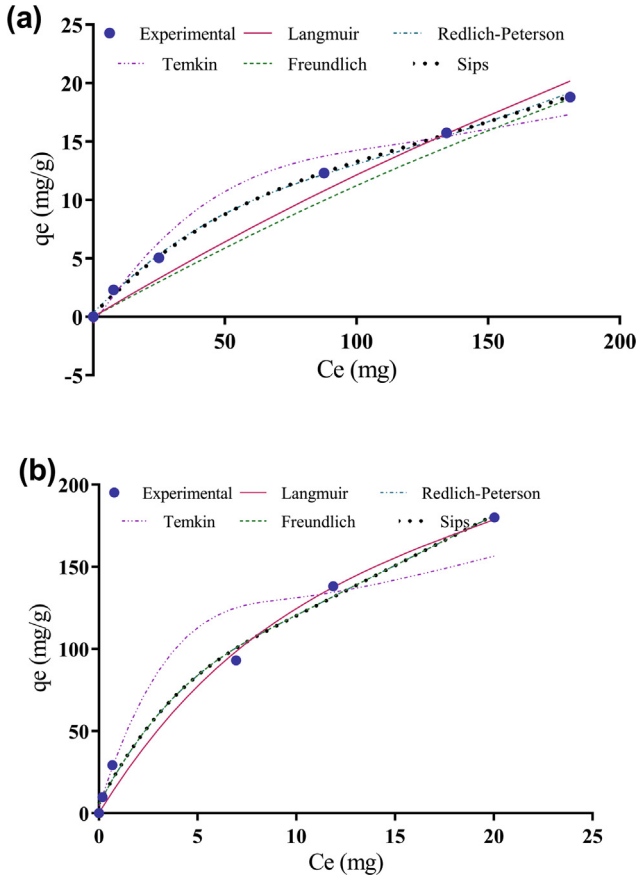

Fig. 8. Investigation of tetracycline adsorption isotherm by Clinoptilolite adsorbent (a) and Fe_3O_4/Clinoptilolit nanocomposite (b).

In Table 4, the maximum adsorption capacity (q_{max}) of several similar adsorbents in different studies has been shown; the q_{max} of the nanocomposite Fe_3O_4/Clinoptilolite according to Freundlich isotherm is 180.9 (mg/g), which is considered to be highly efficient compared to other similar adsorbents and nanocomposite (Table 4). In the study of Babaei et al., the removal of TC by magnetic hydroxyapatite was more in line with the Langmuir isotherm, and the maximum adsorption capacity was 64.5 mg/g [38], which did not agree with the findings of this study. Kakavandi et al. used magnetic activated carbon adsorbent with Fe_3O_4 particles to remove the residual amoxicillin and found that the removal process of this drug was proportional to the Langmuir and Freundlich isotherms and reached a maximum contaminant adsorption capacity of 136.98 mg/g [47], which is consistent with the findings of this study.

3.6. Adsorption kinetics

To express the results of kinetic studies, two parameters of correlation coefficient (R^2) and root-mean-square error (RMSE) are mainly used, which were calculated through Eqs. (16) and (17).

$$R^2 = 1 - \frac{\sum_{n=1}^{n}\left(q_{t.exp.n} - q_{t.cal.n}\right)^2}{\sum_{n=1}^{n}\left(q_{t.exp.n} - \bar{q}_{t.exp.n}\right)^2} \quad (16)$$

$$\mathrm{RMSE} = \sqrt{\frac{1}{n+1}\sum_{n=1}^{n}\left(q_{t.exp.n} - q_{t.exp.n}\right)^2} \quad (17)$$

In these equations, $q_{t.exp.n}$ and $q_{t.cal.n}$ are the amount of adsorption capacity at time t and in the actual values of the experiments and the values predicted by the model, respectively. N also refers to the number of experiments. The results of kinetic calculations of the pseudo-first, pseudo-second, and Elovich models were shown in Table S4. According to the values of correlation coefficient (R^2) and RMSE, it is observed that the adsorption process of the contaminant (tetracycline) by both Fe_3O_4/Clinoptilolit and Clinoptilolite adsorbents is consistent with pseudo-first and pseudo-second kinetic models for all initial concentrations of contaminants (10, 30, 100, 150, and 200 mg/L). However, the data does not fit with the Elovich kinetic model at some initial concentrations of the contaminant (100 and 200 mg/L). Moreover, The correlation coefficient (R^2) of the pseudo-first kinetic model (PFO) for all concentrations is higher than that of R^2 of the pseudo-second

kinetic model (PSO), and its RMSE is less than that of the pseudo-second model (PSO) (Fig. 8). Furthermore, the maximum adsorption capacity (q_m) of all contaminant concentrations (tetracycline) is closer to the maximum adsorption capacity (q_m) of the pseudo-first-order model (PFO), and the contaminant adsorption process by these two adsorbents is in agreement with the pseudo-first-order kinetic model (PFO). It shows that the diffusion occurs from inside a layer and is based on the solid adsorption capacity and the changes in the adsorption rate per unit time are proportional to the number of unoccupied adsorption sites in the adsorbent surface.

Changes in the amount of pollutant adsorption by both adsorbents mentioned in the unit of time can be seen in Fig. 9. As known, the rate of adsorption of pollutants by both adsorbents is initially high, and the highest adsorption of pollutant (TC) occurs in the first 40 min. In general, the high slope of kinetic diagrams shows the amount of highly adsorbed contaminants on different levels of adsorbents studied at the beginning of the work, which is balanced with a delay of 40 min; this high adsorption rate is due to free and unoccupied adsorption sites in the beginning. The decrease in adsorption rate after equilibrium time may be due to the diffusion of TC molecules and the occupation of nanocomposite pores, which prevents the adsorption of contaminants by the nanosorbent.

3.7. Thermodynamics

The results of experiments and thermodynamic calculations were shown in Table 5. According to the negative values of standard free energy (ΔG^0) for all mentioned temperatures, the process of adsorption of pollutants by Fe_3O_4/Clinoptilolite adsorbent can be done spontaneously (feasibility), which is consistent with the study of Zhaohui Li et al. conducted for removal of TC from aqueous solutions by kaolinite [48]. The value of ΔH^0 is equal to −54.91, which indicates that the process of adsorption of the pollutant is exothermic. The results of this part of the study are consistent with the results of research by Tizro, Saeed et al.; they found that the removal of heavy metals by nanomagnetic adsorbent from aqueous solution is exothermic [49]. Moreover, the obtained negative standard entropy ($\Delta S°$) also specifies a reduction in the irregularities in the common phase of solid and liquid (adsorbent and solution), which leads to a decrease in the removal rate of the contaminant (tetracycline) due to an increase in temperature; this is in agreement with result of Zhaohui Li et al. in the removal of tetracycline from aqueous solutions by kaolinite [48]. The results of this part of this research project (H^0 and $0 > \Delta S^\circ$) do not correspond to the results of the study of Yu, Runqiang et al. in the removal of chlortetracycline by modified zeolite from aqueous solutions [50].

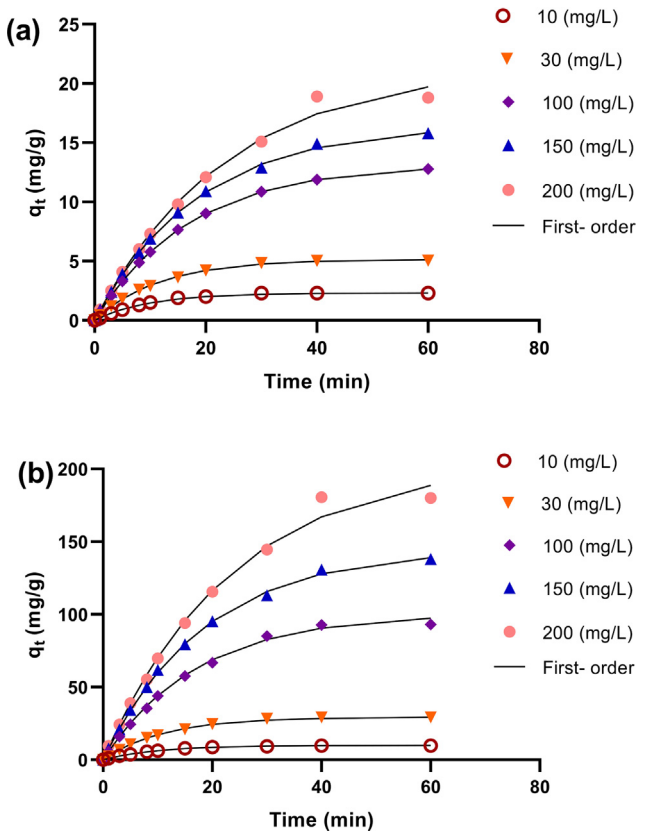

Fig. 9. Adsorption kinetics for tetracycline adsorption by Clinoptilolite adsorbent (a) and Fe_3O_4/Clinoptilolit nanocomposite (b).

3.8. Adsorption mechanism

TC is an amphoteric organic substance whose basic framework is the molecular polycyclic tetraphenyl carboxamide due to the simultaneous presence of both weak bases of the weak dimethyl amino base group and the weakly acidic phenolic hydroxyl group, as well as the keto and enol functional groups containing the double bond [51].

According to the pH of the solution, TC in aqueous solutions is observed in the forms of (a) TCH_3^+ at pH < 3.3,(b) TCH_2° at 3.3 < pH < 7.7, (c) TCH^- at 7.7 < pH < 9.7, and (d) TC^{2-} at pH > 9.7 [11], and the pH of the zero point (pHzpc) of Fe_3O_4/Clinoptilolite adsorbent is 6.2, which is in the range of pH of 5.5 to 6.5 as observed in other studies [36,37]. It indicates that the electric charge of the nanocomposite surface is positive and protonated in the range of less than this pH and is negative above this range.

Very low adsorption capacity at acidic pH, due to the predominance of H^+ ions in solution, hydrogen bonds between H^+ and ions derived from the TC polar molecule causes the formation of electrostatic repulsion between ions with same charge derived from the TC molecule and functional groups on the surface of Fe_3O_4/Clinoptilolite nanocomposite; this consequently reduces the adsorption capacity of tetracycline by Fe_3O_4/Clinoptilolite nanocomposite in acidic conditions [51] (Fig. 10). In the neutral pH range, hydrogen bonding between tetracycline ions (TCH_2°) and OH functional groups on the surface of Fe_3O_4/Clinoptilolite nanocomposite is converted into the main driving force for the adsorption of pollutants by the nanocomposite and leads to observe the highest removal efficiency at pH of 7 and 8. In addition, the increase in adsorption capacity in neutral conditions is related to the highly hydrophobic nature of zutrion species (TCH_2°) of the tetracycline molecule in hydrophobic reactions and bonding with nanocomposite functional groups. With increasing pH in alkaline ion conditions, the negative ions of TC (anions) predominate in pH solution of 9; due to the negative charges on the nanocomposite surface, it leads to an electrostatic repulsion force between the homonymous (negative-negative) charges and more decrease in removal efficiency decreases [38,51,52].

3.9. Investigation of the effect of interfering ions in the adsorption process

Since different waters have different concentrations of different anions and cations that can affect the adsorption process, the effect of ions was studied using different concentrations of NaCl and constant conditions including contaminant concentration of 50 mg/L, adsorbent dose of 1 g/L and pH of 8. The results of this part of study were shown in the diagrams of Fig. 11a. As can be seen in NaCl concentration of 0 M, the efficiency of Fe_3O_4/Clinoptilolite nanocom-

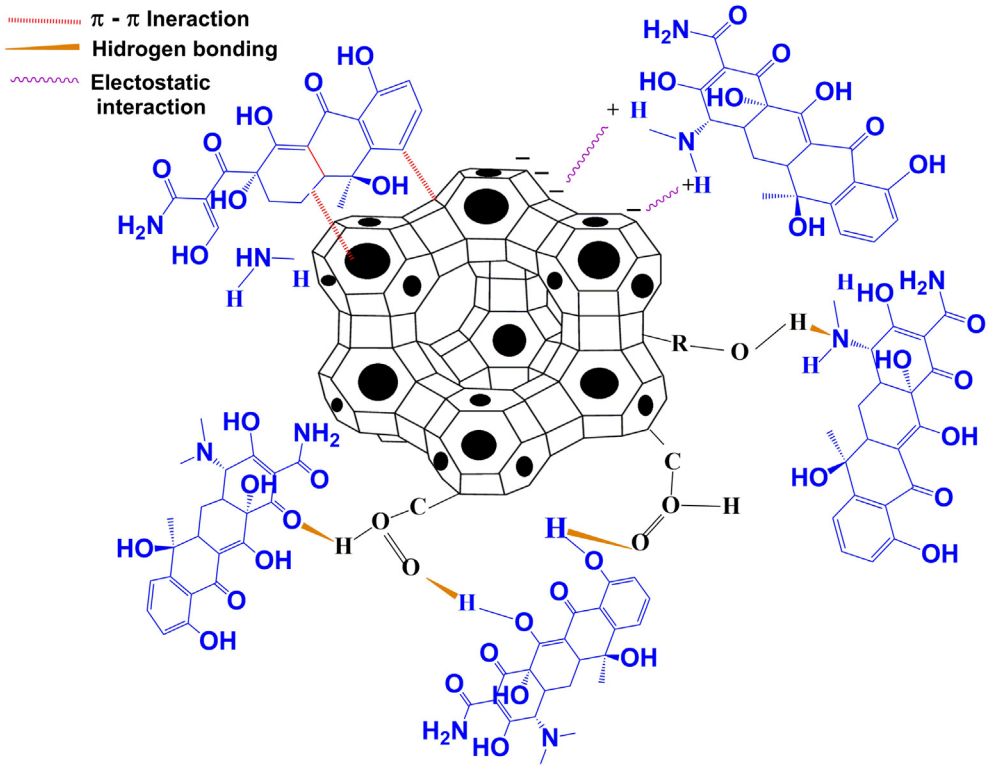

Fig 10. Adsorption mechanism of tetracycline using Fe_3O_4/Clinoptilolit nanocomposite.

posite in removing tetracycline contaminant was 96.1% and in NaCl concentration of 0.01 M, 94.05% of TC was removed by Fe_3O_4/Clinoptilolite nanocomposite. Moreover, at concentrations of 0.05 and 0.1 M, 92.5 and 91.1% of TC were removed by Fe_3O_4/Clinoptilolite nanocomposite, respectively, and at NaCl concentrations of 0.3 M and 0.5 M, TC removal efficiencies by Fe_3O_4/Clinoptilolite nanocomposites were 86.5% and 61.2%, respectively. According to mentioned results, it can be concluded that the rate of reduction in removal efficiency by Fe_3O_4/Clinoptilolite at concentrations of 0.01, 0.05, 0.1, 0.3 M of NaCl was not significant. However, at a concentration of 0.5 M of NaCl, the removal efficiency of the contaminant by nanocomposite is 61.2%. This amount of reduction in removal of TC at a concentration of 0.5 M NaCl can be due to the occupation of adsorption sites by ions derived from NaCl, which prevents the adsorption and removal of contaminants by the nanocomposite.

3.10. Reusabilty of Fe_3O_4/Clinoptilolite adsorbent

In order to reduce costs and protect the environment, it is necessary to pay attention to the reuse of the synthesized adsorbent. For this purpose, for adsorbent recycling, the rate of tetracycline adsorption and reuse of Fe_3O_4/Clinoptilolite adsorbent used were investigated in successive cycles. At the end of each step, the nanocomposite was separated from the solution by a magnet and washed several times with distilled water and ethanol and dried in an oven at 50 °C for 24 h. The evaluation results of five reuse of the nanocomposite at pH of 8, adsorbent dose of 1 g/L, and contaminant concentration of 50 mg/L were shown in Fig. 11b. In the first and second stages, 96.01 and 95.3% of the pollutants were removed, respectively, and in the third, fourth and fifth stages, 93.18, 80.6 and 27.03% of the pollutants were removed, respectively. This reduction in contaminant removal efficiency can be related to the reduction of adsorption sites on the adsorbent and the loss of adsorbent after each recovery cycle. These results show

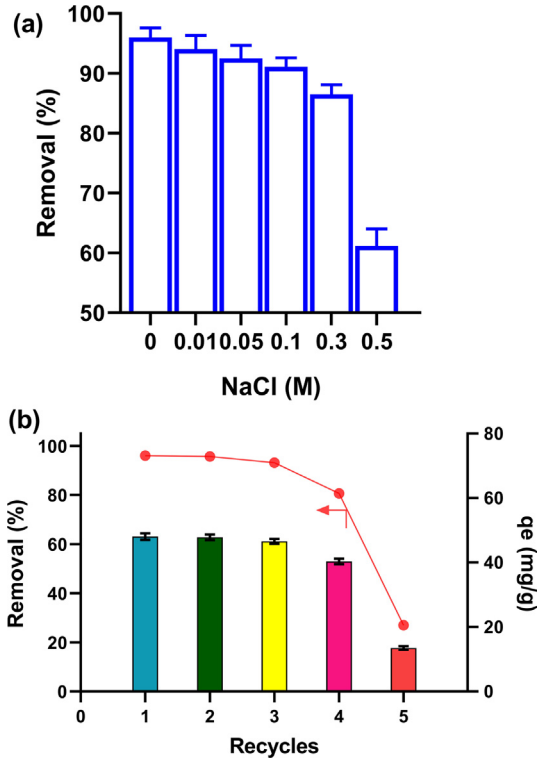

Fig. 11. Effect of different concentrations of NaCl on the removal of tetracycline (a), and adsorbent reusability (b) (adsorbent dose of 1 gr/L, tetracycline concentration of 50 mg /L and pH of 8).

that Fe_3O_4/Clinoptilolite adsorbent can be used four times with high efficiency to remove contaminants and prevent the entry of new contaminants into the environment and have a significant

impact on reducing the cost of contaminant treatment from contaminated environments.

4. Conclusion

In the present study, the structure and properties of Fe_3O_4/Clinoptilolite nanocomposite and Clinoptilolite adsorbents were identified by VSM, FTIR, EDAX, SEM, and XRD methods. Mentioned adsorbents were employed for the removal of tetracycline (TC) from aqueous solutions to investigate their ability. In the studies, the removal processes by Fe_3O_4/Clinoptilolite and Clinoptilolite adsorbents were more consistent with Freundlich and Langmuir isotherms, respectively. Moreover, in kinetic studies, the results were more consistent with pseudo-first-order kinetics. The highest removal efficiencies were obtained at pH values of 7 and 8. In nanocomposite reuse tests, it was found that after several steps, Fe_3O_4/Clinoptilolite nanocomposites could provide high contaminant removal efficiency. In thermodynamic studies, the standard free energy (ΔG^0) was negative at different temperatures, indicating spontaneity and applicability of the process. Moreover, the standard enthalpy value (ΔH^0) and standard entropy value (ΔS^0) were −54.91 and −0.15, respectively, indicating exothermic adsorption process and reduction of irregularity in the liquid phase. The effect of disturbing ions on the adsorption process was investigated at different concentrations of NaCl, and it was detected that different concentrations of NaCl have no significant effect on the TC adsorption process by nanocomposites. Therefore, considering these conditions, Fe_3O_4/Clinoptilolite nanocomposite can be used to remove antibiotic contaminants from water sources.

CRediT authorship contribution statement

Mehdi Rouhani: Data curation, Writing – original draft. **Seyed Davoud Ashrafi:** Visualization, Investigation, Supervision. **Kamran Taghavi:** Supervision. **Mohammad Naimi Joubani:** Software, Validation. **Jalil Jaafari:** Conceptualization, Methodology, Software.

Declaration of Competing Interest

The authors declare that they have no known competing financial interests or personal relationships that could have appeared to influence the work reported in this paper.

Acknowledgements

This paper was supported financially by a grant (No. 99082601) from the Research Center of Health and Environment, Guilan University of Medical Sciences, Rasht, Iran.

Appendix A. Supplementary material

Supplementary data to this article can be found online at https://doi.org/10.1016/j.molliq.2022.119040.

References

[1] A. Azari, M. Salari, M.H. Dehghani, M. Alimohammadi, H. Ghaffari, K. Sharafi, N. Shariatifar, M. Baziar, J. Maz. Univ. Med. Sci. 26 (2017) 265.
[2] K. Sharafi, M. Pirsaheb, V.K. Gupta, S. Agarwal, M. Moradi, Y. Vasseghian, E.-N. Dragoi, J. Mol. Liq. 274 (2019) 699.
[3] D.J. Naghan, A. Azari, N. Mirzaei, A. Velayati, F.A. Tapouk, S. Adabi, M. Pirsaheb, K. Sharafi, Bul. Chem. Commun. 47 (2015) 14.
[4] J.L. Martinez, Environ. Pollut 157 (2009) 2893.
[5] D. Naghipour, L. Hoseinzadeh, K. Taghavi, J. Jaafari, A. Amouei, Int. J. Environ. Anal. Chem. (2021) 1.
[6] A. Dehghan, A. Zarei, J. Jaafari, M. Shams, A.M. Khaneghah, Chemosphere 217 (2019) 250.
[7] D. Naghipour, K. Taghavi, J. Jaafari, I. Kabdaşlı, M. Makkiabadi, M.J.M. Doust, F.J. M. Doust, Environ. Technol. (2021) 1.
[8] D. Naghipour, L. Hoseinzadeh, K. Taghavi, J. Jaafari, Data Br. 18 (2018) 1082.
[9] T. Pirom, T. Wongsawa, T. Wannachod, N. Sunsandee, U. Pancharoen, S. Kheawhom, Chem. Papers 71 (2017) 1291.
[10] Y. Zhao, J. Geng, X. Wang, X. Gu, S. Gao, J. Colloid Interface Sci. 361 (2011) 247.
[11] Y. Dai, J. Li, D. Shan, Chemosphere 238 (2020) 124432.
[12] H. Darmokoesoemo, F. Setianingsih, T. Putranto, H. Kusuma, Rasayan J. Chem. 9 (2016) 550.
[13] R.A. Khera, M. Iqbal, A. Ahmad, S.M. Hassan, A. Nazir, A. Kausar, H.S. Kusuma, J. Niasr, N. Masood, U. Younas, Desalin. Water Treat. 201 (2020) 289.
[14] A. Badeenezhad, A. Azhdarpoor, S. Bahrami, S. Yousefinejad, Mol. Simul. 45 (2019) 564.
[15] A. Badeenezhad, A. Azhdarpoor, Desalin Water Treat 154 (2019) 347.
[16] H. Hao, G. Liu, Y. Wang, B. Shi, K. Han, Y. Zhuang, Y. Kong, J. Hazard. Mater. 362 (2019) 246.
[17] A.H. Lu, E.E.L. Salabas, F. Schüth, Angew. Chem 46 (2007) 1222.
[18] X.X. Liang, A. Omer, Z.-H. Hu, Y.G. Wang, D. Yu, X.-K. Ouyang, Chemosphere 217 (2019) 270.
[19] A.A. Amooey, A. Amouei, H. Tashakkorian, S.N. Mohseni, J. Maz. Univ. Med. Sci. 25 (2016) 128.
[20] H.S. Kusuma, A. Ansori, S. Wibowo, D.S. Bhuana, M. Mahfud, Korean Chem. Eng. Res. 56 (2018) 435.
[21] H.S. Kusuma, A.N. Amenaghawon, H. Darmokoesoemo, Y.A. Neolaka, B.A. Widyaningrum, C.L. Anyalewechi, P.I. Orukpe, Environ. Technol. Innovat. 24 (2021) 102005.
[22] J. Jaafaria, K. Yaghmaeiana, Desalin. Water Treat. 142 (2019) 225.
[23] A. Karami, K. Karimyan, R. Davoodi, M. Karimaei, K. Sharafie, S. Rahimi, T. Khosravi, M. Miri, H. Sharafi, A. Azari, Desalin. Water Treat. 89 (2017) 150.
[24] M. Pirsaheb, M. Moradi, H. Ghaffari, K. Sharafi, Int. J. Pharm. Technol. 8 (2016) 11023.
[25] D. Naghipour, K. Taghavi, M. Ashournia, J. Jaafari, R. Arjmand Movarrekh, Water Environ. J. 34 (2020) 45.
[26] S.D. Ashrafi, G.H. Safari, K. Sharafi, H. Kamani, J. Jaafari, Int. J. Biol. Macromol. (2021).
[27] V.D. Nguyen, T.T. Pham, V. Vranova, H.T. Nguyen, L.T. Nguyen, X.T. Vuong, Q.M. Bui, Environ. Technol. Innovat. 20 (2020) 101166.
[28] Y. Wei, B. Han, X. Hu, Y. Lin, X. Wang, X. Deng, Proc. Eng 27 (2012) 632.
[29] M. Sabonian, K. Mahanpoor, Arch. Hyg. Sci. 10 (2021) 1.
[30] A. Mollahosseini, M. Toghroli, Asian J. Sci. Res. 5 (2015) 120.
[31] V. Alimohammadi, F. Kashanian, S. Seyyed Ebrahimi, M. Habibi Rezaei, A. Bagherpour, Metal. Eng. 21 (2018) 275.
[32] M. Mahmoodi Meimand, N. Javid, M. Malakootian, Health Scope 8 (2019).
[33] V. Javanbakht, S.M. Ghoreishi, N. Habibi, M. Javanbakht, Powder Technol. 302 (2016) 372.
[34] L.-Y. Zhang, X.-J. Zhu, H.-W. Sun, G.-R. Chi, J.-X. Xu, Y.-L. Sun, Curr. Appl Phys. 10 (2010) 828.
[35] J. Jaafari, H. Barzanouni, S. Mazloomi, N.A.A. Farahani, K. Sharafi, P. Soleimani, G.A. Haghighat, Int. J. Biol. Macromol. 164 (2020) 344.
[36] M. Gharloghi, A. Yazdanbakhsh, A. Eslami, E. Aghayani, J. Maz. Univ. Med. Sci. 26 (2016) 130.
[37] Q. Liu, L.-B. Zhong, Q.-B. Zhao, C. Frear, Y.-M. Zheng, A.C.S. Appl, Mater. Interfaces 7 (2015) 14573.
[38] A.A. Babaei, K. Ahmadi, I. Kazeminezhad, S.N. Alavi, A. Takdastan, J. Maz. Univ. Med. Sci. 26 (2016) 146.
[39] M.M. Ali, M. Ahmed, B. Hameed, J. Clean. Prod. 172 (2018) 602.
[40] S.M. Mirsoleimani-azizi, P. Setoodeh, S. Zeinali, M.R. Rahimpour, J. Environ. Chem. Eng. 6 (2018) 6118.
[41] J. Perić, M. Trgo, N.V. Medvidović, Water Res. 38 (2004) 1893.
[42] A. Peyghami, A. Moharrami, Y. Rashtbari, S. Afshin, M. Vosuoghi, A. Dargahi, J. Dispersion Sci. Technol. (2021) 1.
[43] B. Acenioglu, J. Colloid Interface Sci. 274 (2004) 371.
[44] B.A. Fil, M. Yilmaz, S. Bayar, M. Elkoca, Braz. J. Chem. Eng. 31 (2014) 171.
[45] L.M. Camacho, R.R. Parra, S. Deng, J. Hazard. Mater. 189 (2011) 286.
[46] S. Mohseni, A. Amooey, H. Tashakkorian, A. Amouei, Int. J. Environ. Sci. Technol. 13 (2016) 2261.
[47] B. Kakavandi, A. Esrafili, A. Mohseni-Bandpi, A. Jonidi Jafari, R. Rezaei Kalantary, Water Sci. Technol. 69 (2014) 147.
[48] Z. Li, L. Schulz, C. Ackley, N. Fenske, J. Colloid Interface Sci. 351 (2010) 254.
[49] S. Tizro, H. Baseri, J. Adv. Mat. Process 4 (2016) 15.
[50] R. Yu, X. Yu, B. Xue, J. Liao, W. Zhu, S. Tian, J. Environ. Sci. Health A 55 (2020) 573.
[51] X. Zhang, X. Lin, Y. He, Y. Chen, X. Luo, R. Shang, Int. J. Biol. Macromol. 124 (2019) 418.
[52] X. Bao, Z. Qiang, J.-H. Chang, W. Ben, J. Qu, J. Environ. Sci. 26 (2014) 962.
[53] C.P. Okoli, A.E. Ofomaja, J. Clean. Prod. 217 (2019) 42.
[54] J. Kang, H. Liu, Y.-M. Zheng, J. Qu, J.P. Chen, J. Colloid Interface Sci. 344 (2010) 117.
[55] A.A. Mohammed, T.J. Al-Musawi, S.L. Kareem, M. Zarrabi, A.M. Al-Ma'abreh, Arab. J. Chem. 13 (2020) 4629.
[56] J. Dai, X. Meng, Y. Zhang, Y. Huang, Bioresour. Technol 311 (2020) 123455.